Characterization of Adenosine-A1 Receptor–Mediated Antilipolysis in Rats by Tissue Microdialysis, ^{1}H-Spectroscopy, and Glucose Clamp Studies

Corinna Schoelch, Johanna Kuhlmann, Matthias Gossel, Guenter Mueller, Claudia Neumann-Haefelin, Ulrich Belz, Juergen Kalisch, Gabriele Biemer-Daub, Werner Kramer, Hans-Paul Juretschke, and Andreas W. Herling

Increased supply of fatty acids to muscle and liver is causally involved in the insulin resistance syndrome. Using a tissue microdialysis technique in Wistar and Zucker fatty (ZF) rats, we determined tissue glycerol levels as a marker of lipolysis in gastrocnemius muscle (gMT), subcutaneous adipose (SAT), and visceral adipose tissue (VAT) as well as the reduction of plasma free fatty acids, glycerol, and triglycerides caused by the antilipolysis-specific adenosine-A1 receptor agonist (ARA). In Wistar and ZF rats, ARA significantly lowered dialysate glycerol levels in SAT, VAT, and gMT. Whereas in SAT and VAT the decrease in dialysate glycerol indicated adipocytic antilipolysis, this decrease in gMT was not caused by a direct effect of ARA on intramyocellular lipolysis, as demonstrated by the lack of inhibition of the protein kinase A activity ratio in gMT. In addition, no differences of the fed-starved-refed dynamics of intramyocellular triglyceride levels compared with untreated controls were measured by in vivo ^{1}H-spectroscopy, excluding any adenylate cyclase–independent antilipolysis in muscle. Treatment with ARA resulted in pronounced reductions of plasma free fatty acids, glycerol, and triglycerides. Furthermore, in ZF rats, ARA treatment caused an immediate improvement of peripheral insulin sensitivity measured by the euglycemic-hyperinsulinemic glucose clamp technique. ***Diabetes*** **53:1920–1926, 2004**

Adipose tissue is increasingly being recognized as a complex organ with a host of endocrine and paracrine functions that affect an array of metabolic and other functions (1). Although it seems histologically almost homogeneous, it is functionally heterogeneous, depending mainly on the anatomic location of the adipose tissue. Adipose depots differ in their cellular structure (2), biochemical properties in vitro (3), and metabolism in vivo in both humans and rodents (4,5). Many genetic and environmental factors can induce changes in structure and function of adipose tissue with one of the most critical outcomes being the accumulation of excess fat mass leading to obesity and insulin resistance.

Insulin resistance is defined as an impaired ability of this hormone to suppress hepatic glucose output and to promote peripheral glucose disposal (6). Skeletal muscle is a major locus for insulin resistance, playing a key role in whole-body glucose homeostasis. A common feature of insulin-resistant conditions is elevated levels of circulating free fatty acids (FFAs) (7), which oppose the effect of insulin on glucose homeostasis (8). The source of circulating FFAs and glycerol is the adipose tissue compartment in which triglycerides (TGs) are stored and hydrolyzed. Several recent studies have shown that there is also lipolytic activity of skeletal muscle tissue in vivo (9,10). Furthermore, differences in glycerol release among different muscle types that seem to be related to muscle fiber composition have been detected (11). The important role of intramyocellular TGs (IMTGs) in the pathogenesis of insulin resistance is further demonstrated by studies showing a negative relationship between IMTGs and whole-body insulin sensitivity in both humans and rodents (12–14). IMTGs correlate more tightly with insulin resistance than any of the other commonly measured parameters (6). However, muscle TGs themselves do not seem to interfere directly with insulin action in the myocytes but rather impair insulin signaling through some other fatty acid–derived metabolite, e.g., long-chain acyl-CoAs.

Endogenous adenosine is supposed to be an important regulator of adipose tissue metabolism by increasing the sensitivity of adipocyte glucose transport and oxidation and by inhibiting lipolysis potently. Lipolysis is triggered by adenosine-A1 receptors (15–17). Therefore, selective adenosine-A1-agonists have been suggested to be useful as antilipolytic drugs in the treatment of type 2 diabetes. By suppressing lipolysis, they could decrease plasma FFA and TG levels (18–21).

The aim of the present study was to investigate the antilipolytic activity of the antilipolysis-specific adenosine-A1 receptor agonist (ARA) by the tissue microdialysis technique in gastrocnemius muscle (gMT), subcutaneous adipose (SAT), and visceral adipose tissue (VAT) of Wistar

From Aventis Pharma Deutschland, Frankfurt am Main, Germany.

Address correspondence and reprint requests to Dr. Andreas W. Herling, Disease Group Metabolic Diseases, Pharmacology H 815/H 821, Aventis Pharma Deutschland, Industriepark Hoechst, 65926 Frankfurt/Main, Germany. E-mail: andreas.herling@aventis.com.

Received for publication 27 May 2003 and accepted in revised form 27 March 2004.

C.S. is currently affiliated with Boehringer Ingelheim, Biberach, Germany.

ARA, adenosine-A1 receptor agonist; FFA, free fatty acid; GIR, glucose infusion rate; gMT, gastrocnemius muscle tissue; HSL, hormone-sensitive lipase; IMTG, intramyocellular TG; mLPL, muscle lipoprotein lipase; MRS, magnetic resonance spectroscopy; PKA, protein kinase A; SAT, subcutaneous adipose tissue; SOL, *m. soleus*; TG, triglyceride; TIB, *m. tibialis*; VAT, visceral adipose tissue.

and obese Zucker fatty (ZF) rats. Magnetic resonance spectroscopy (MRS) studies were performed to monitor intramyocellular lipolysis. In addition, glucose clamp studies were performed to determine the acute effect of ARA on insulin sensitivity in ZF rats.

RESEARCH DESIGN AND METHODS

Male Wistar rats (450–500 g; HsdCpb:Wu; Charles River) and insulin-resistant male obese ZF rats (700–1100 g; CRL:(Zuc)-fa; Charles River) were used for the experiments. The animals were fed with SSNIFF pellet chow (Soest, Germany) and water ad libitum. They were kept at 22°C, 60% relative humidity on a 12-h light-dark cycle.

Test compound. ARA ([1S,2R,3R,5R]-3-methoxymethyl-5-[6-(1-[5-trifluoromethyl-pyridin-2-yl]pyrrolidin-3-[S]-ylamino)-purin-9-yl]cyclopentane-1,2-diol; molecular formula, $C_{22}H_{26}F_3N_7O_3$; molecular weight, 493.49) is an antilipolysis-specific ARA, without any hemodynamic effects at antilipolytic doses, synthesized by the chemical department at Aventis. ARA is highly selective for rat and human A1 (K_i = 16 nmol/l), compared with A2a (K_i >100,000 nmol/l), A2b (K_i >100,000 nmol/l), and A3 (K_i >9,000 nmol/l) receptors. Functionally, it is a potent antilipolytic agent (inhibition of isoproterenol- and adenosine deaminase–induced lipolysis in isolated rat adipocytes: IC_{50} = 11 nmol/l) but has no effect on heart rate (rat right atria: IC_{50} >100,000 nmol/l), making it essentially a partial agonist in the heart but a full agonist in the adipocyte. ARA was suspended in 0.5% methylcellulose in saline and administered at the dose of 10 mg/kg intraperitoneally. Vehicle was administered to control rats.

All experimental procedures were conducted according to the German Animal Protection Law. Tissue microdialysis and euglycemic-hyperinsulinemic glucose clamp studies were performed after an overnight fast in anesthetized rats. Anesthesia was achieved by a bolus injection of pentobarbital at a dose of 60 mg/kg intraperitoneally and maintained by a subcutaneous infusion of ~20 $mg \cdot kg^{-1} \cdot h^{-1}$. Rats were tracheotomized, and peripheral veins were prepared for blood collections or infusions. Body temperature was kept at 37°C using a heating pad.

The determination of the protein kinase A (PKA) activity ratio was determined in overnight starved Wistar rats 15 or 60 min after administration of ARA. Cytosol fractions were prepared from SAT, VAT, and gMT excised from the anesthetized animals and assayed for PKA specific activity ratio.

ARA was administered in tissue microdialysis studies after a baseline period of 2 h. In glucose clamp studies, rats received ARA twice, at 16 h before the study and 1 h before the insulin infusion. In the MRS study, IMTG was determined on day 1 during normal fed conditions, on day 2 after an overnight fast, and on day 3 after refeeding. On day 2 after the second MRS measurement, eight rats received ARA; the other rats served as controls for the IMTG determination on day 3.

Tissue microdialysis. Changes of glycerol concentrations in the intercellular space of the examined tissue regions were determined using microdialysis, as described in detail elsewhere (22). Briefly, the day before a microdialysis experiment, microdialysis catheters (CMA/20; membrane, Polycarbonat; cut off, 20,000 D; Solna, Sweden) were rinsed with Ringer solution (10–12 h) to remove the glycerol coat of the probe. Microdialysis catheters were inserted into SAT, VAT, and gMT. These tissues were then perfused using microdialysis pumps (CMA 100 or CMA 102; Microdialysis AB, Stockholm, Sweden) at a speed of 2 μl/min with Ringer solution plus 50 mmol/l ethanol for the evaluation of hemodynamic changes. During the first hour, no dialysate was collected to allow stabilization of glycerol levels. Dialysate fractions were then collected every 30 min up to 7 h and were immediately analyzed for dialysate glycerol and ethanol. At the end, the animals were killed by pentobarbital overdose, and the correct location of the probes was visually proved.

Changes in blood flow were determined by using the ethanol dilution technique, which is based on Fick's principle (23,24). As ethanol readily diffuses through the probe membrane and is not metabolized by peripheral tissues, an escape from the perfusion medium to the extracellular compartment measured by the ethanol outflow/inflow ratio would be dependent on blood flow in the tissue surrounding the microdialysis probe (23,25). The method has been accepted as a good indicator of small variations in the nutritive blood flow to the tissue surrounding the microdialysis probe, and it gives comparable results to those obtained by the ^{133}Xe-clearance technique (24). A decrease in the $[ethanol]_{dialysate}/[ethanol]_{perfusate}$ ratio is equivalent to an increase in blood flow and vice versa.

Blood samples were drawn from the jugular veins for determination of FFAs, glycerol, and TGs at time points indicated in the figures. The blood samples were placed in K-EDTA tubes and centrifuged at 5,400*g* for 4 min at 4°C.

MRS. In vivo MRS studies in anesthetized Wistar rats were performed on a 7 Tesla Biospec system (Bruker BioSpin, Ettlingen, Germany) as described previously (12,26). Briefly, IMTG was determined in the *m. tibialis* (TIB) and *m. soleus* (SOL), via volume-selective ^{1}H-MR spectroscopy, and expressed as IMTG/tCr ratio.

Euglycemic-hyperinsulinemic glucose clamp study. The experimental procedure was performed as described previously (12).

Determination of PKA activity ratio. Frozen tissue samples were minced under liquid N_2 in 2 ml of 25 mmol/l morpholinoethanesulfonic acid (pH 6.0), 140 mmol/l NaCl, 2 mmol/l EDTA, 0.5 mmol/l EGTA, 0.25 mol/l sucrose, 50 mmol/l NaF, 10 mmol/l sodium pyrophosphate, 20 mmol/l glycerol-3-phosphate, 1 mmol/l sodium orthovanadate, 2 μmol/l microcystin LR, 1 μmol/l okadaic acid, and protease inhibitors per gram of wet weight and then homogenized by sequential use of an Ultraturrax homogenizer (30 s, maximum speed) and a Teflon-in-glass homogenizer (tightly fitting, five strokes, 3,000 rpm, on ice). After centrifugation (500*g*, 5 min, 4°C), the infranatant below the fat layer was carefully removed, adjusted to 0.5% Triton X-100, and after incubation (30 min, 4°C) and homogenization (Teflon-in-glass, 10 strokes, 500 rpm, 4°C) centrifuged (10,000*g*, 15 min, 4°C). The supernatant was re-centrifuged (100,000*g*, 1 h, 4°C). Twenty-five microliters of the supernatant (cytosol) were incubated (30 min, 30°C) with 12.5 μl of assay buffer (200 mmol/l Tris/HCl [pH 7.5], 40 mmol/l $MgCl_2$, 4 mmol/l ATP, 400 μmol/l rhodamine-labeled kemptide [PepTag A1 peptide obtained from Serva/Promega Heidelberg, Germany]) in the absence or presence of 10 μmol/l mono-butyryl-cAMP and 50 μmol/l heat-stable PKA inhibitor peptide (Sigma, Deisenhofen, Germany) in a total volume of 50 μl. The reaction was terminated by placing the tube into a boiling water bath for 2 min, and the mixture was stored at −20°C for further analysis. Portions of this mixture (10 μl) supplemented with 1 μl of 80% glycerol were separated by agarose gel electrophoresis (0.8% in 50 mmol/l Tris/HCl [pH 8.0], 15 min at 100 V). Phosphorylated kemptide (net charge −1) migrating toward the anode and separated from the nonphosphorylated species (net charge +1) moving toward the cathode were visualized under UV light. For quantitative evaluation, the gel material that contained the phosphorylated band was excised (125 μl), heated (95°C), and supplemented with 75 μl of gel solubilization solution and 50 μl of glacial acetic acid, and finally its absorbance was determined at 570 nm using a 96-well plate reader (normalized for liquefied agarose containing no kemptide). The PKA activity ratio was calculated as the ratio between the absorbance in the absence and presence of cAMP corrected in each case for unspecific phosphorylation in the presence of the PKA inhibitor (which was <15% of total) and reflects the portion of PKA activity (i.e., cAMP concentration) present at the time point of removal of the tissue samples. Control experiments demonstrated that the activity ratio is independent of dilution of the tissue homogenate (and protein concentration) from 2 g wet wt/ml to 0.03 g/ml (limit of detection) and of incubation period (up to 2 h), thereby excluding formation of inactive PKA dephosphorylated holoenzyme during homogenization and subsequent assay.

Analytical procedures. During the tissue microdialysis experiment, dialysate glycerol was measured with an automated analyser (CMA 600, CMA Microdialysis AB) using an enzymatic fluorometric method. In situ recoveries were found to be 33% for dialysate glycerol at near equilibrium (27). Ethanol was determined in the perfusate (inflow) and dialysate (outflow) with the biochemistry analyzer YSI 2700 Select (Kreienbaum, Germany).

Standard procedures were used to determine blood parameters for glucose, FFAs, glycerol, and TGs (28). Plasma insulin concentrations were assayed with a radioimmunoassay kit obtained from Linco (St. Charles, MO).

Statistical analysis. The program Sigma Stat 2.0 (Jandel, Erkrath, Germany) was used for multifactorial ANOVA, including factor repetition when required. Average data values were described by least square means (± SE) provided by ANOVA.

RESULTS

Tissue microdialysis. During the 2-h baseline period, glycerol levels were constant in all tissues. The mean baseline glycerol concentrations of the three examined tissues in both rat strains are shown in Fig. 1. The comparison of the baseline levels in Wistar rats revealed significant differences in dialysate glycerol levels of the examined tissues in contrast to ZF rats. Their glycerol levels were not different between the examined tissues and were significantly higher than those of Wistar rats.

Using the ethanol dilution technique as an indirect marker for tissue blood flow, it was confirmed that blood flow had stabilized 1 h after insertion of the catheters and

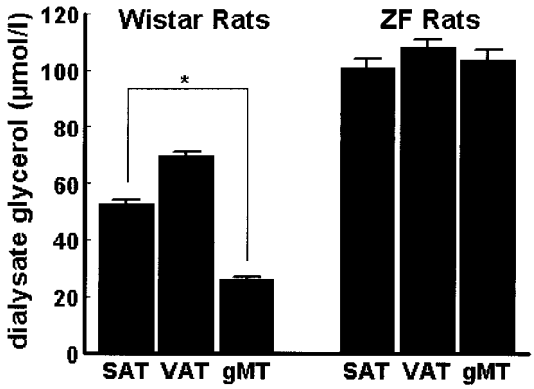

FIG. 1. Comparison of the mean dialysate glycerol levels during the 2-h baseline period in SAT, VAT, and gMT of Wistar (n = 14–19) and ZF (n = 10–14) rats. Values are mean ± SE. *P < 0.001 for the differences between the tissues. All values were significantly different between the two rat strains for the respective tissue.

remained stable over the time course of the microdialysis experiment (2 h baseline plus 5 h after ARA administration; data not shown). The comparison of the baseline ethanol ratio reveals clear differences between the examined tissues. In Wistar rats, the lowest ethanol ratio was found in gMT (0.48 ± 0.02), indicating a significantly higher blood supply compared with both adipose tissues (SAT, 0.58 ± 0.02; VAT, 0.70 ± 0.02; $P < 0.001$, comparison between the different tissues). It is interesting that the ethanol ratio found in SAT and VAT of ZF rats was slightly but significantly elevated compared with the blood flow in adipose tissue of Wistar rats (SAT, 0.84 ± 0.02; VAT, 0.79 ± 0.02; $P < 0.001$, comparison between both adipose tissues in the different rat strains), indicating a decreased blood flow in SAT and VAT of ZF rats compared with Wistar rats. In gMT, no significant differences in the ethanol ratio and, therefore, in blood flow could be detected between the two different rat strains (0.52 ± 0.02).

Acute treatment with ARA significantly lowered dialysate glycerol levels in all three tissues examined, in both Wistar and ZF rats (Fig. 2). The mean glycerol reduction in Wistar rats was 30.1 ± 3.4, 27.4 ± 4.3, and 16.9 ± 1.4 µmol/l in SAT, VAT, and gMT, respectively ($P < 0.001$, compared with their own baseline levels). Glycerol levels of vehicle-treated control Wistar rats remained stable in all tissues during the whole experiment. In ZF rats, the decrease of dialysate glycerol levels caused by ARA was more pronounced with a mean glycerol reduction of 64.4 ± 9.5, 45.1 ± 7.6, 58.8 ± 9.0 µmol/l in SAT, VAT, and gMT, respectively ($P < 0.05$, compared with their own

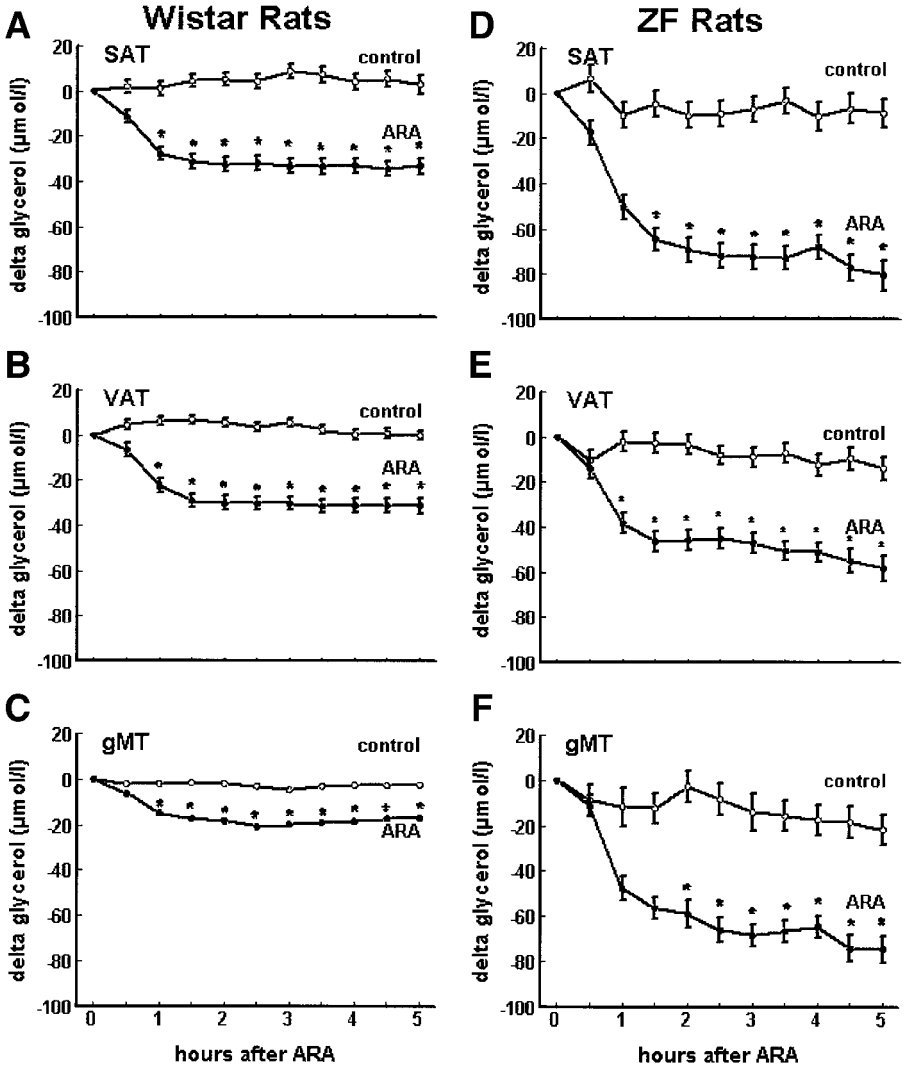

FIG. 2. Absolute decreases from the baseline values of the respective tissues of dialysate glycerol in SAT (A and D), VAT (B and E), and gMT (C and F) after acute treatment with ARA in Wistar (A–C; n = 6–12) and ZF (D–F; n = 5–8) rats. Values are mean ± SE. *P < 0.05 vs. control.

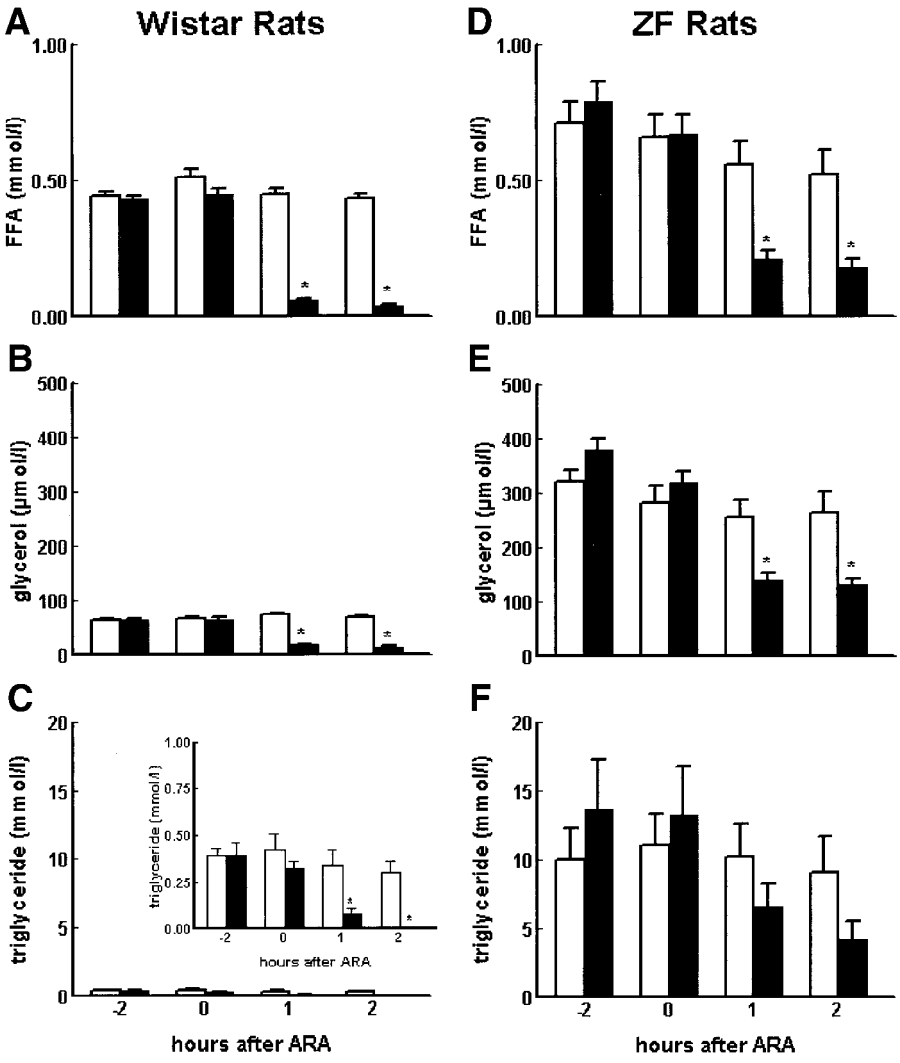

FIG. 3. Effect of ARA (■) on plasma FFAs (*A* and *D*), glycerol (*B* and *E*), and TGs (*C* and *F*) in Wistar (*A–C*; $n = 8–12$) and ZF (*D–F*; $n = 8$) rats. The inset in *C* represents plasma TGs of Wistar rats with a different scaling because of their low levels. Values are mean ± SE. *$P < 0.05$ vs. respective control (□).

baseline levels). The glycerol levels of vehicle-treated ZF rats showed also a slight decrease compared with their baseline values of ~6.4 ± 10.6, 7.9 ± 7.4, and 13.1 ± 12.1 µmol/l for SAT, VAT, and gMT, respectively, during the experiment, but this did not reach statistical significance (Fig. 2).

In Wistar as well as in ZF rats, treatment with ARA did not cause any changes in the ethanol ratio, indicating that there was no effect of ARA on circulation in the examined tissues (data not shown). The reduction of dialysate glycerol levels was therefore due to an ARA-mediated inhibition of lipolysis rather than to an increased transport of glycerol because of changes in the capillary blood flow.

In the tissue microdialysis study, blood levels of FFAs, glycerol, and TGs were significantly reduced in ARA-treated Wistar rats by 90, 78, and 98%, respectively, compared with control animals (Fig. 3). In comparison with Wistar rats, ZF rats already showed slightly elevated FFA, 5-fold elevated glycerol, and 25-fold elevated TG levels during the baseline period. ARA treatment reduced FFAs, glycerol, and TGs in ZF rats by 60, 50, and 55%, respectively (Fig. 3).

PKA activity ratios. To clarify whether these powerful effects on plasma lipids and tissue glycerol were indeed caused by activation of adenylate cyclase-cAMP-PKA signaling cascade, we investigated the effect of ARA on PKA activation in SAT, VAT, and gMT 15 and 60 min after administration of ARA to Wistar rats. ARA caused a significant reduction of the PKA activity ratio, which monitors the portion of cAMP-stimulated autophosphorylated PKA, in SAT and VAT within 15 min, which remained significantly reduced in VAT but not in SAT for 60 min. These results presumably reflect different time courses of homologous desensitization of the adenosine receptor A1 and/or downstream signaling by ARA. However, in gMT, there was no effect on the PKA activity ratio (Table 1). From these results, we conclude that ARA inhibited lipolysis via inhibition of adenylate cyclase-cAMP-PKA pathway in SAT and VAT but did not cause cAMP-mediated intramyocellular antilipolysis.

MRS. Recently, we identified that starvation-induced adipocytic lipolysis occurred in parallel to increased TG formation in glycolytic (TIB) and intermediary (*m. extensor digitorum longus*) muscles but not in oxidative muscle (SOL) (26). However, on refeeding starvation-mediated elevated IMTGs in TIB decreased immediately, which is consistent with intramyocellular lipolysis. Therefore, in 24-h-starved rats as used for microdialysis studies, no net intramyocellular lipolysis can be expected during baseline conditions. However, cAMP-independent mechanisms of

TABLE 1
PKA activity ratios in SAT and VAT as well as in gMT of overnight starved Wistar rats, 15 and 60 min after administration of ARA at a dose of 10 mg/kg or vehicle, respectively

	PKA activity ratios		
	SAT	VAT	gMT
Control			
15 min	0.35 ± 0.04	0.43 ± 0.05	0.14 ± 0.02
60 min	0.35 ± 0.06	0.41 ± 0.06	0.14 ± 0.04
ARA			
15 min	0.16 ± 0.02†	0.13 ± 0.02†	0.14 ± 0.02
60 min	0.40 ± 0.06	0.23 ± 0.02*	0.13 ± 0.04

Data are means ± SE (n = 8 each group). *$P < 0.05$, †$P < 0.001$ vs. respective control group.

antilipolysis caused by adenosine (via the adenosine-A1 receptor) have been described (15,29). To assess such cAMP-independent ARA-mediated antilipolysis in muscle, we investigated the dynamics of IMTGs in TIB and SOL by in vivo ^{1}H-MRS on refeeding after a 24-h fast. IMTGs in TIB increased after starvation for 24 h, and ARA treatment did not prevent the decrease of IMTGs on refeeding, indicating that ARA did not affect intramyocellular lipolysis (Table 2). The IMTG content in SOL did not change during the entire experiment, which is consistent with previously published results (26).

Euglycemic-hyperinsulinemic glucose clamp. To examine the effect of ARA treatment on the insulin-resistant condition of ZF rats, we determined whole-body insulin sensitivity using the glucose clamp technique. ZF rats displayed marked insulin resistance compared with Wistar rats, demonstrated by a lower glucose infusion rate (GIR) and by elevated levels of plasma FFAs, which were not as suppressible during insulin infusion as in Wistar rats (Table 3). Therefore, a significantly diminished insulin-mediated antilipolysis occurred during hyperinsulinemia (insulin infusion rate 4.8 $mU \cdot kg^{-1} \cdot min^{-1}$), reflected by a significantly reduced GIR in ZF rats compared with Wistar rats. Acute treatment with ARA clearly improved whole-body insulin sensitivity in ZF rats accompanied by a significant increase in GIR compared with untreated animals under glucose-clamp conditions. The treatment also led to a significant decrease of plasma FFA levels at basal conditions and during insulin infusion, decreasing to levels measured in Wistar rats. Plasma glycerol and TG levels were also significantly reduced after ARA treatment (Table 3).

DISCUSSION

In this study, we investigated the antilipolytic properties of ARA in different adipose and muscle tissues and examined the positive effects of the treatment on plasma lipid parameters and whole-body insulin sensitivity. By using the entry of glycerol from the extracellular space into dialysate as a marker for lipolysis, these experiments demonstrate the potent ARA-mediated inhibition of adipocytic lipolysis by significantly reducing interstitial glycerol levels in all tissues examined in Wistar and even more pronounced in obese ZF rats. Because ARA treatment caused no changes in nutritive blood flow, the reduction of glycerol levels are due to an inhibition of lipolysis in both adipose tissues, which is accompanied by an decrease in blood plasma glycerol and FFAs. Reduction of plasma FFA levels causes a reduced supply of FFAs to the liver, thus limiting hepatic reesterification to TGs and resulting in an overall reduction of circulating plasma TG levels. This improvement of the plasma lipid profile in obese ZF rats resulted in an increase in whole-body insulin sensitivity as demonstrated by the hyperinsulinemic-euglycemic glucose clamp study.

Because of a ubiquitous peripheral distribution of the A1-receptor, separation of the desirable effects from unwanted effects is difficult for A1-receptor agonists (30). The severe bradycardiac and hypotensive action of adenosine receptor agonists (31) seemed to limit the use of these agonists for other therapeutic areas. However, recent studies showed that low-efficacy agonists for the adenosine-A1 receptor cause antilipolysis with negligible or no effects on the cardiovascular system (32–34). Therefore, the specificity of ARA on antilipolysis can be explained by its weak agonistic A1-receptor properties, exclusively displaying a strong antilipolytic effect without any hemodynamic effects.

The general mechanism by which adenosine inhibits lipolysis is via activation of the A1-receptor, linked to reduced cAMP formation (35) and inhibition of PKA and finally of hormone-sensitive lipase (HSL) activity. In addition, it has been shown that adenosine (via the adenosine-A1 receptor) affects lipolysis by cAMP-independent mechanisms (15,29). The reduced PKA activity after ARA treatment was demonstrated in SAT and VAT but not in gMT, indicating that ARA-mediated antilipolysis occurred in adipocytes but not in muscle cells. In addition, the drop in IMTG levels after refeeding in TIB of control and ARA-treated rats revealed that ARA has no effect on intramyocellular lipolysis and excluded any cAMP-independent antilipolytic effects of ARA in muscle tissue.

The microdialysis experiments also demonstrate marked differences in dialysate glycerol levels between two different adipose depots (SAT, VAT) and gMT in Wistar rats under baseline conditions. Regional differences in the regulation of adipose tissue metabolism have been well documented and are mainly due to different adrenergic receptor expression and activation (36,37). Because

TABLE 2
In vivo ^{1}H-MRS data for IMTG/tCr in TIB and SOL in fed, 24-h starved, and refed Wistar rats

	Control fed (n = 15)	Control 24-h starved (n = 15)	Control refed (n = 7)	ARA refed (n = 8)
IMTG (TIB)	0.23 ± 0.02	0.31 ± 0.02*	0.20 ± 0.04	0.18 ± 0.02
IMTG (SOL)	0.49 ± 0.04	0.45 ± 0.04	0.54 ± 0.08	0.44 ± 0.07

Data are means ± SE (n = 7–15). *$P < 0.05$ vs. fed. Before refeeding (after 24 h of starvation), one subgroup of rats (ARA; n = 8) was treated with ARA at the dose of 10 mg/kg.

TABLE 3
Mean values of GIR, FFAs, glycerol, TGs, and plasma insulin during euglycemic-hyperinsulinemic glucose clamp studies in ZF (control versus ARA treated) and Wistar rats (control)

	Insulin infusion ($mU \cdot kg^{-1} \cdot min^{-1}$)	GIR ($mg \cdot kg^{-1} \cdot min^{-1}$)	FFAs (mmol/l)	Glycerol (μmol/l)	TGs (mmol/l)	Insulin (ng/ml)
ZF	0	0	0.81 ± 0.04	339 ± 14	3.3 ± 0.3	8.1 ± 0.5
Control	4.8	2.3 ± 0.4	0.54 ± 0.03	339 ± 25	3.5 ± 0.4	13.8 ± 1.3
ZF	0	0	0.51 ± 0.09†	87 ± 9	1.7 ± 0.3*§	1.9 ± 0.1*
ARA	4.8	8.5 ± 0.3*‡	0.05 ± 0.01†	80 ± 8	1.2 ± 0.2*§	13.8 ± 0.6‡
Wistar	0	0	0.48 ± 0.03†	64 ± 4*	0.3 ± 0.1*	1.3 ± 0.4*
Control	4.8	16.1 ± 0.7*	0.05 ± 0.01†	19 ± 3*	0.2 ± 0.1*	3.9 ± 0.7*

Data are means ± SE ($n = 8$). *$P < 0.001$, †$P < 0.05$ vs. ZF control; ‡$P < 0.001$, §$P < 0.05$ vs. Wistar control.

the ethanol ratio was significantly lower in SAT compared with VAT and the concentration of a particular substance in the extracellular space depends on blood flow and on cell metabolism (24), this may reflect the existence of a reduced fluid drainage in epididymal adipose tissue. Therefore, vascular characteristics of the adipose tissue depots could mask a difference in basal lipolysis, resulting in a less prominent difference between the two adipose compartments (38).

However, for muscle tissue, the origin of glycerol is more complex than for adipose tissue. Several in vivo studies in humans have shown that there is an active lipolytic process within skeletal muscle with a significant release (9,10) but also with an uptake of glycerol (39,40). However, in a recent human study, an overnight fast induced a significant net release of glycerol, especially from the gastrocnemius muscle, which exhibits a relative dominance of oxidative type 1 fibers in comparison with other muscles (11). Recently, we demonstrated by ^{1}H-MRS technique in rats that IMTGs in the oxidative SOL muscle did not change despite drastic elevations of FFA levels during starvation, whereas in glycolytic (TIB) and intermediary muscles, an intramyocellular TG formation occurred in parallel to adipocytic lipolysis (26). On refeeding, elevated IMTGs in glycolytic and intermediary muscles immediately dropped to normal fed values, consistent with intramyocellular lipolysis. Therefore, in 24-h starved rats as used for microdialysis studies, no net intramyocellular lipolysis could be expected. We assume that the major part of glycerol in muscle tissue under baseline conditions may be due to intravascular TG hydrolysis by muscle lipoprotein lipase (mLPL). This is supported by studies showing an elevated mLPL activity during starvation (41,42).

The obese ZF rat represents an animal model for insulin resistance and obesity. In this model, tissue-specific differences in glycerol levels vanished. As the differences in glycerol levels between the two rat strains are, at least in muscle tissue, not due to differences in blood flow, the dramatic increase in tissue glycerol in all examined tissues reflects enhanced lipolytic activity. Applying the microdialysis technique, we cannot distinguish whether this higher lipolysis is due to a higher activity of either HSL or lipoprotein lipase under fasting conditions. In addition, muscle tissue of ZF rats possesses a greater number of adipocytes interspersed between the muscle fibers, and it therefore may be possible that the lipolytic activity of extramyocellular lipids from intramuscular adipose tissue contributes significantly to the interstitial glycerol pool in muscle in this animal model. The elevated glycerol levels found in both adipose tissues could partly be explained by differences in the ethanol ratio compared with Wistar rats, as a marked reduction in blood flow would hamper the removal of glycerol from tissue. A decreased blood flow in SAT was also observed in obese humans (43–45) and may be due to various tissue parameters such as the size of adipocytes, differences in the organization and permeability of the connective web, and the density of microvessels surrounding the microdialysis probe (46). However, a higher basal lipolytic activity of adipocytes derived from ZF rats was also shown in cell culture experiments (47).

In summary, our studies demonstrate a marked reduction of plasma FFAs and glycerol, reflecting in vivo inhibition of lipolysis in adipocytes after administration of ARA. Reduction of plasma FFA levels has far-reaching consequences by reducing the supply of FFAs to the liver, thus limiting hepatic reesterification to TGs and resulting in an overall reduction of circulating plasma TG levels. The antilipolytic properties of ARA were further demonstrated by a massive lowering of tissue glycerol levels without causing changes in microcirculation. As confirmed by the glucose clamp study, the inhibition of lipolysis by ARA treatment markedly improved insulin sensitivity and glucose uptake in insulin-resistant ZF rats and is therefore suggested as a useful new therapeutic principle for the treatment of lipid disorders combined with insulin resistance.

REFERENCES

1. Mohamed-Ali V, Pinkney JH, Coppack SW: Adipose tissue as an endocrine and paracrine organ. *Int J Obes Relat Metab Disord* 22:1145–1158, 1998
2. Pond CM: Some conceptual and comparative aspects of body composition analysis. In *Techniques in the Behavioural Sciences.* Toates FM, Rowland NE, Eds. Amsterdam, Elsevier Scientific, 1987, p. 499–529
3. Fried SK, Lavau M, Pi-Sunyer FX: Variations of glucose metabolism by fat cells from three adipose depots of the rat. *Metabolism* 31:876–883, 1982
4. Arner P: Differences in lipolysis between human subcutaneous and omental adipose tissues. *Ann Med* 27:435–438, 1995
5. Pond CM, Mattacks CA: The effects of noradrenaline and insulin on lipolysis in adipocytes isolated from nine different adipose depots of guinea-pigs. *Int J Obes* 15:609–618, 1991
6. McGarry JD: Banting lecture 2001: dysregulation of fatty acid metabolism in the etiology of type 2 diabetes. *Diabetes* 51:7–18, 2002
7. Reaven GM, Hollenbeck C, Jeng CY, Wu MS, Chen YD: Measurement of plasma glucose, free fatty acid, lactate, and insulin for 24 h in patients with NIDDM. *Diabetes* 37:1020–1024, 1988
8. Boden G: Role of fatty acids in the pathogenesis of insulin resistance and NIDDM. *Diabetes* 46:3–10, 1997
9. Maggs DG, Jacob R, Rife F, Lange R, Leone P, During MJ, Tamborlane WV, Sherwin RS: Interstitial fluid concentrations of glycerol, glucose, and amino acids in human quadricep muscle and adipose tissue: evidence for significant lipolysis in skeletal muscle. *J Clin Invest* 96:370–377, 1995
10. Bolinder J, Kerckhoffs DA, Moberg E, Hagstrom-Toft E, Arner P: Rates of

skeletal muscle and adipose tissue glycerol release in nonobese and obese subjects. *Diabetes* 49:797–802, 2000
11. Hagstrom-Toft E, Qvisth V, Nennesmo I, Ryden M, Bolinder H, Enoksson S, Bolinder J, Arner P: Marked heterogeneity of human skeletal muscle lipolysis at rest. *Diabetes* 51:3376–3383, 2002
12. Kuhlmann J, Neumann-Haefelin C, Belz U, Kalisch J, Juretschke HP, Stein M, Kleinschmidt E, Kramer W, Herling AW: Intramyocellular lipid and insulin resistance: a longitudinal in vivo 1H-spectroscopic study in Zucker diabetic fatty rats. *Diabetes* 52:138–144, 2003
13. Phillips DI, Caddy S, Ilic V, Fielding BA, Frayn KN, Borthwick AC, Taylor R: Intramuscular triglyceride and muscle insulin sensitivity: evidence for a relationship in nondiabetic subjects. *Metabolism* 45:947–950, 1996
14. Krssak M, Falk Petersen K, Dresner A, DiPietro L, Vogel SM, Rothman DL, Roden M, Shulman GI: Intramyocellular lipid concentrations are correlated with insulin sensitivity in humans: a 1H NMR spectroscopy study. *Diabetologia* 42:113–116, 1999
15. Kuroda M, Honnor RC, Cushman SW, Londos C, Simpson IA: Regulation of insulin-stimulated glucose transport in the isolated rat adipocyte: cAMP-independent effects of lipolytic and antilipolytic agents. *J Biol Chem* 262:245–253, 1987
16. Martin SE, Bockman EL: Adenosine regulates blood flow and glucose uptake in adipose tissue of dogs. *Am J Physiol* 250:H1127–H1135, 1986
17. Heseltine L, Webster JM, Taylor R: Adenosine effects upon insulin action on lipolysis and glucose transport in human adipocytes. *Mol Cell Biochem* 144:147–151, 1995
18. Hoffman BB, Chang H, Dall'Aglio E, Reaven GM: Desensitization of adenosine receptor-mediated inhibition of lipolysis: the mechanism involves the development of enhanced cyclic adenosine monophosphate accumulation in tolerant adipocytes. *J Clin Invest* 78:185–190, 1986
19. Fredholm BB: Effect of adenosine, adenosine analogues and drugs inhibiting adenosine inactivation on lipolysis in rat fat cells. *Acta Physiol Scand* 102:191–198, 1978
20. Wieser PB, Pendleton TS: Effects of an N6-disubstituted adenosine derivative (BM 11.189) on fat cell metabolism. *Biochem Pharmacol* 28:693–694, 1979
21. Strong P, Anderson R, Coates J, Ellis F, Evans B, Gurden MF, Johnstone J, Kennedy I, Martin DP: Suppression of non-esterified fatty acids and triacylglycerol in experimental animals by the adenosine analogue GR79236. *Clin Sci (Lond)* 84:663–669, 1993
22. Benveniste H, Huttemeier PC: Microdialysis—theory and application. *Prog Neurobiol* 35:195–215, 1990
23. Fellander G, Linde B, Bolinder J: Evaluation of the microdialysis ethanol technique for monitoring of subcutaneous adipose tissue blood flow in humans. *Int J Obes Relat Metab Disord* 20:220–226, 1996
24. Enoksson S, Nordenstrom J, Bolinder J, Arner P: Influence of local blood flow on glycerol levels in human adipose tissue. *Int J Obes Relat Metab Disord* 19:350–354, 1995
25. Hickner RC, Rosdahl H, Borg I, Ungerstedt U, Jorfeldt L, Henriksson J: The ethanol technique of monitoring local blood flow changes in rat skeletal muscle: implications for microdialysis. *Acta Physiol Scand* 146:87–97, 1992
26. Neumann-Haefelin C, Beha A, Kuhlmann J, Belz U, Gerl M, Quint M, Biemer-Daub G, Broenstrup M, Stein M, Kleinschmidt E, Schaefer HL, Schmoll D, Kramer W, Juretschke HP, Herling AW: Muscle-type specific intramyocellular and hepatic lipid metabolism during starvation in Wistar rats. *Diabetes* 53:528–534, 2004
27. Kehr J: Measuring in vivo recovery in microdialysis—when do we need it? *Microline* 2:6–7, 1996
28. Bergmeyer HU: *Methoden der Enzymatischen Analyse.* Weinheim, Verlag Chemie, 1974
29. Londos C, Honnor RC, Dhillon GS: cAMP-dependent protein kinase and lipolysis in rat adipocytes. III. Multiple modes of insulin regulation of lipolysis and regulation of insulin responses by adenylate cyclase regulators. *J Biol Chem* 260:15139–15145, 1985
30. Jacobson KA, van Galen PJ, Williams M: Adenosine receptors: pharmacology, structure-activity relationships, and therapeutic potential. *J Med Chem* 35:407–422, 1992
31. Olsson RA, Pearson JD: Cardiovascular purinoceptors. *Physiol Rev* 70: 761–845, 1990
32. Mathot RA, Van der Wenden EM, Soudijn W, IJzerman AP, Danhof M: Deoxyribose analogues of N6-cyclopentyladenosine (CPA): partial agonists at the adenosine A1 receptor in vivo. *Br J Pharmacol* 116:1957–1964, 1995
33. Van Der Graaf PH, Van Schaick EA, Math-ot RA, IJzerman AP, Danhof M: Mechanism-based pharmacokinetic-pharmacodynamic modeling of the effects of N6-cyclopentyladenosine analogs on heart rate in rat: estimation of in vivo operational affinity and efficacy at adenosine A1 receptors. *J Pharmacol Exp Ther* 283:809–816, 1997
34. van Schaick EA, de Greef HJ, Langemeijer MW, Sheehan MJ, IJzerman AP, Danhof M: Pharmacokinetic-pharmacodynamic modelling of the antilipolytic and anti-ketotic effects of the adenosine A1-receptor agonist N6-(p-sulphophenyl)adenosine in rats. *Br J Pharmacol* 122:525–533, 1997
35. Klinger M, Freissmuth M, Nanoff C: Adenosine receptors: G protein-mediated signalling and the role of accessory proteins. *Cell Signal* 14:99–108, 2002
36. Arner P, Hellstrom L, Wahrenberg H, Bronnegard M: Beta-adrenoceptor expression in human fat cells from different regions. *J Clin Invest* 86:1595–1600, 1990
37. Hellmer J, Marcus C, Sonnenfeld T, Arner P: Mechanisms for differences in lipolysis between human subcutaneous and omental fat cells. *J Clin Endocrinol Metab* 75:15–20, 1992
38. Portillo MP, Villaro JM, Torres MI, Macarulla MT: In vivo lipolysis in adipose tissue from two anatomical locations measured by microdialysis. *Life Sci* 67:437–445, 2000
39. Frayn KN, Coppack SW, Humphreys SM: Glycerol and lactate uptake in human forearm. *Metabolism* 40:1317–1319, 1991
40. Coppack SW, Persson M, Judd RL, Miles JM: Glycerol and nonesterified fatty acid metabolism in human muscle and adipose tissue in vivo. *Am J Physiol* 276:E233–E240, 1999
41. Ladu MJ, Kapsas H, Palmer WK: Regulation of lipoprotein lipase in adipose and muscle tissues during fasting. *Am J Physiol* 260:R953–R959, 1991
42. Cortright RN, Muoio DM, Dohm GL: Skeletal muscle lipid metabolism: a frontier for new insights into fuel homeostasis. *Nutr Biochem* 8:228–245, 1997
43. Blaak EE, van Baak MA, Kemerink GJ, Pakbiers MT, Heidendal GA, Saris WH: Beta-adrenergic stimulation and abdominal subcutaneous fat blood flow in lean, obese, and reduced-obese subjects. *Metabolism* 44:183–187, 1995
44. Jansson PA, Larsson A, Smith U, Lonnroth P: Glycerol production in subcutaneous adipose tissue in lean and obese humans. *J Clin Invest* 89:1610–1617, 1992
45. Summers LK, Samra JS, Humphreys SM, Morris RJ, Frayn KN: Subcutaneous abdominal adipose tissue blood flow: variation within and between subjects and relationship to obesity. *Clin Sci (Lond)* 91:679–683, 1996
46. Millet L, Barbe P, Lafontan M, Berlan M, Galitzky J: Catecholamine effects on lipolysis and blood flow in human abdominal and femoral adipose tissue. *J Appl Physiol* 85:181–188, 1998
47. Vannucci SJ, Klim CM, Martin LF, LaNoue KF: A1-adenosine receptor-mediated inhibition of adipocyte adenylate cyclase and lipolysis in Zucker rats. *Am J Physiol* 257:E871–E878, 1989